Profilin–Actin Complexes Directly Elongate Actin Filaments at the Barbed End†

M. Pring,‡ A. Weber,*,§ and M. R. Bubb‖

Departments of Physiology and of Biochemistry and Biophysics, University of Pennsylvania, Philadelphia, Pennsylvania 19104, and Laboratory of Cell Biology, National Heart, Lung and Blood Institute, National Institutes of Health, Bethesda, Maryland 20892

Received April 29, 1991; Revised Manuscript Received October 2, 1991

ABSTRACT: We demonstrate that the profilin–G-actin complex can elongate actin filaments directly at the barbed end but cannot bind to the pointed end. During elongation, the profilin–actin complex binds to the barbed filament end, whereupon profilin is released, leaving the actin molecule behind. This was first proposed by Tilney [Tilney, L. G., et al. (1983) *J. Cell Biol. 97*, 112–124] and demonstrated by Pollard and Cooper [(1984) *Biochemistry 23*, 6631–6641] by electron microscopy. We show that a model without any outside energy supply, in contrast to the mechanism proposed by Pollard and Cooper, can be fitted to our and their [Kaiser et al. (1986) *J. Cell Biol. 102*, 221–226] findings. Input of outside energy is necessary only if profilin-mediated elongation continues after free G-actin has been lowered to or below the critical concentration observed at the barbed end in the absence of profilin.

Most nonmuscle cells contain a high concentration of monomeric actin although the critical concentration of actin is very low in ionic media comparable to cytoplasm [cf. Korn (1982) and Pollard and Cooper (1986)]. The monomeric actin in excess of the critical concentration is not incorporated into actin filaments because it is sequestered by monomer binding proteins. Examples in mammalian cells are profilin, discovered by Lindberg (Carlson et al., 1977) and extensively studied by Korn (Reichstein & Korn, 1979; Mockrin & Korn, 1980; Tobacman & Korn, 1982; Tobacman et al., 1983; Lal & Korn, 1985) and by Pollard (Tseng & Pollard, 1982; Tseng et al., 1984; Pollard & Cooper, 1984, 1986; Kaiser et al., 1986), the 5-kilodalton protein thymosin β4, recently discovered in platelets (Safer et al., 1990, 1991), and actin depolymerizing factor or destrin (Bamberg et al., 1980; Moriyama et al., 1990) which is closely related to actophorin (Cooper et al., 1986) and depactin (Mabuchi, 1983) in lower organisms. Other proteins, such as actobindin from *Acanthamoeba* (Lambooy & Korn, 1986; Vandekerckhove et al., 1990; Bubb & Korn, 1991; Bubb et al., 1991), may sequester a fraction of the unpolymerized actin in oligomeric structures.

Upon stimulation, some cells like neutrophils or platelets rapidly convert about half of this unpolymerized actin into F-actin (Fechheimer & Zigmond, 1983; Wallace et al., 1984; Devriotes & Zigmond, 1988; Casella et al., 1981; Fox & Phillips, 1981). The data in this paper relate to a regulatory mechanism that has the potential to affect the rate of this redistribution of actin. Tilney (Tilney et al., 1983) was the first to point out that one needs to find an explanation why the rate of elongation at the barbed filament end can be very high, although practically all of the cellular G-actin is sequestered by monomer binding proteins and the free G-actin concentration is quite low. The rate of acrosome elongation in *Thyone* is much higher than can be accounted for by the steady-state concentration of free G-actin, which is maximally 0.5 μM, if nearly all barbed filament ends are capped. Tilney proposed that the complex between G-actin and profilin, the major monomer sequestering protein in *Thyone*, associates directly, at a diffusion-limited rate, with the barbed filament ends. Binding of the complex is followed by the immediate release of free profilin which leaves behind the actin molecule, thus causing rapid elongation.

Pollard and his colleagues (Pollard & Cooper, 1984; Kaiser et al., 1986), applying electron microscopy to an in vitro system, presented quantitative data indicating that the profilin-bound actin directly elongates the barbed, but not the pointed end. In contrast, Lal and Korn (1985), using light scattering to observe filament elongation, reported elongation rates at the barbed end proportional to the free G-actin concentration, which suggests that the profilin-bound actin did not contribute to filament elongation.

When considering regulation, it is important to be certain whether or not profilin–actin complexes could contribute significantly to filament elongation at the barbed end. A very rapid rate of elongation—of which the acrosome elongation in *Thyone* is an extreme example—would otherwise require a monomer concentration very much higher than the maximal steady-state G-actin concentration of 0.5 μM which could sustain an elongation rate of only about 0.8 μm/min. The rate would be 40–80 times higher if the profilin–actin complex, which could have a concentration of 20–40 μM according to the measurements of total profilin by Lind et al. (1987) and by Southwick and Young (1990), could directly participate in filament elongation. Otherwise, a faster rate of filament elongation would require the rapid release of free G-actin by some kind of regulatory mechanism acting on one of the monomer binding proteins.

We therefore repeated the study of the rate of filament elongation in the presence of profilin, using *Acanthamoeba* proteins, and the fluorescence change of pyrene-labeled actin as the indicator of polymerization. With this method the value for each rate measurement is averaged over a very large number of filaments and can be derived from the data points of the whole time course of elongation since this follows a single exponential. We measured barbed end elongation by using *Limulus* acrosomal false discharges as nuclei. We confirm that the profilin–actin complex binds to barbed ends followed by rapid dissociation of profilin, and our data indicate that

† This research was supported by NIH Grant HL15835 to the Pennsylvania Muscle Institute.

‡ Department of Physiology, University of Pennsylvania.

§ Department of Biochemistry and Biophysics, University of Pennsylvania.

‖ National Institutes of Health.

0006-2960/92/0431-1827$03.00/0

the complex binds with an on-rate constant similar to that of free G-actin.

Materials and Methods

Protein Preparations. *Acanthamoeba* actin was prepared as previously described (Gordon et al., 1977). Pyrenyl actin was prepared according to Kouyama and Mihashi (1981). The critical concentration of two actin preparations varied between 0.08 and 0.035 μM for uncapped and between 0.4 and 0.5 for barbed end capped filaments. *Acanthamoeba* profilin was prepared as previously described (Bubb & Korn, 1991). Acrosomes were isolated from *Limulus* sperm (a generous gift from Tilney) according to Tilney (1975, 1983) with slight modifications as previously described (Young et al., 1990). Gelsolin, a generous gift from J. Bryan, was prepared as previously described (Bryan, 1988).

Protein concentrations were calculated for actin using E_{290} = 24.9 mM^{-1} cm^{-1}, E_{280} = 21.08 for gelsolin, and for profilin 14 mM^{-1} cm^{-1} (Tseng et al., 1984).

Fluorescence and Kinetic Measurements. Changes in actin polymerization were calculated from fluorescence measurements as previously described (Weber et al., 1987a), using a Perkin Elmer MPF-3L.

All experiments were carried out, at 20 °C, with Mg–actin, the physiological form of actin (Weber et al., 1960; Kitasawa et al., 1982) since in a KCl–Mg medium the fluorescence increase of pyrenyl actin starts at the maximal rate with Mg–actin but not with Ca–actin, as first observed by Selden et al. (1983) and shown by Carlier et al. (1986) to be due to the shorter persistence of low fluorescing ATP pyrenyl actin in polymerized Mg–actin as compared to Ca–actin. The conversion to Mg–actin was carried out as previously described (Young et al., 1990).

Measurements of elongation rates at either filament end were carried out as previously described (Walsh et al., 1984; Northrop et al., 1986; Young et al., 1990) in a medium containing 10 mM imidazole buffer, pH 7.4; 0.1 M KCl; 2 mM $MgCl_2$; 1 mM azide; 1 mM dithiothreitol; 0.5 mM ATP; and 1 mM EGTA.

Calculations. (*a*) *Pointed End Controls with 76% Pyrenyl G-Actin.* In all cases *except* barbed end elongation in the presence of profilin [see (e) below], initial rates of fluorescence change due to the addition of pyrenyl G-actin to the pointed, R_p, or barbed ends, R_b, were calculated from the rate constants and amplitudes obtained by fitting the data to single exponentials, using a standard nonlinear optimization routine. These rates were analyzed using the general relationship:

$$R = ak_+n(g + y - c_\infty)y/(g + y) = ak_+ny[1 - c_\infty/(g + y)] \quad (1)$$

where $R = R_p$ or R_b, as defined above; a = molar fluorescence change of conversion of pyrenyl G-actin to pyrenyl F-actin; k_+ = association rate constant for the addition of G-actin to filaments; n = number concentration of filament ends; g = [native G-actin]; y = [pyrenyl G-actin]; and c_∞ = critical concentration. The pointed end controls, in the relevant concentration range, obeyed eq 1. Thus ak_+n and c_∞ were obtained from those at 76% pyrenyl G-actin by simple linear regression of R_p on $(g + y)$.

(*b*) *Pointed End Controls with 8.3% Pyrenyl G-Actin.* Total G-actin was raised by holding pyrenyl G-actin constant and varying native G-actin, so that the percentage of pyrenyl actin ranged over 8.3–40%. This mimics the progressive effect of a binding protein that sequesters native G-actin much more effectively than pyrenyl G-actin. ak_+n and c_∞ were obtained by simple linear regression of R_p on $1/(g + y)$, according to eq 1.

(*c*) *K_d Values for Sequestration of Native and Pyrenyl G-Actin by Profilin.* During the measurements the concentrations of total and pyrenyl actin were held constant while the total concentration of added profilin, $[P]_t$, was varied. Again eq 1 was used, but g and y were obtained from

$$g = g_tK_{dG}/(K_{dG} + [P]) \qquad y = y_tK_{dY}/(K_{dY} + [P]) \quad (2)$$

where g_t = total concentration of native G-actin added; y_t = total concentration of pyrenyl G-actin added; K_{dG} = association constant for profilin sequestration of native G-actin; K_{dY} = association constant for profilin sequestration of pyrenyl G-actin; and [P] = concentration of free profilin. [P] was obtained by solution of the equation:

$$[P][1 + g_t/(K_{dG} + [P]) + y_t/(K_{dY} + [P])] - [P]_t = 0 \quad (3)$$

This was solved numerically by Newton's method, using as a seed the value of [P] estimated, using the applicable quadratic equations, by calculating separately the quantities of native and pyrenyl G-actin that would have been sequestered in the absence of the other, and subtracting their sum from $[P]_t$.

K_{dG} and K_{dY} were obtained by fitting the R_p versus $[P]_t$ relationships observed at both pyrenyl enrichments simultaneously, using a standard nonlinear optimization routine and eq 1, with the values of ak_+n and c_∞ defined by the controls and g and y calculated as outlined above from eqs 2 and 3.

(*d*) *Controls for the Effect of Profilin on the Elongation Rates at the Barbed End.* In view of the importance of the critical concentration, c_∞, in subsequent calculations on the barbed end data, it was obtained separately at 76% pyrenyl G-actin by linear interpolation of null point approximations. Otherwise these barbed end controls were handled similarly to the pointed end controls above, but imposing the null point value of c_∞. In the case of the two sets of data with 5.7% and 2.9% pyrenyl G-actin the critical concentration had clearly drifted overnight from the value obtained the previous day. Therefore, the linear regressions for these data sets were performed simultaneously under the constraints that both lines had the same abscissa intercept and slopes differing by a factor of 2.

(*e*) *Elongation by Profilin–G-Actin Complexes.* The model used is shown in Figure 1. A is either G (native, rate constants k) or Y (pyrenyl, rate constants k'). Equilibrium constants can be defined:

$$k_{1-}/k_{1+} = k'_{1-}/k'_{1+} = c_\infty \qquad k_{2-}/k_{2+} = K_{d2}$$
$$k'_{2-}/k'_{2+} = K'_{d2} \qquad k_{3-}/k_{3+} = K_{d3} \quad (4)$$
$$k'_{3-}/k'_{3+} = K'_{d3}$$

Under the assumption that the net free energy change of filament elongation does not depend on whether it occurs by direct G-actin addition or by G-actin delivery as a profilin complex followed by dissociation of the profilin, the principle of microreversibility (detailed balance, energy square) constrains the equilibrium constants:

$$K_{d3} = c_\infty K_{d2}/K_{dG} \qquad K'_{d3} = c_\infty K'_{d2}/K_{dY} \quad (5)$$

Since the number concentration of filament ends was always much less than the concentrations of other species, their distribution over their possible states was obtained by application of the steady-state assumption to them, and the sequestration

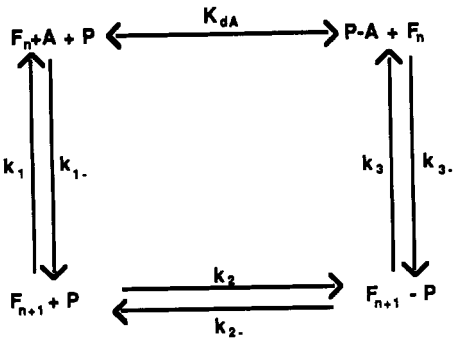

FIGURE 1: Energy square. The reactants at the upper left-hand corner of the square, monomeric actin (A), barbed filament ends (F_n), and profilin (P), are converted to the products, filament ends elongated by one actin monomer (F_{n+1}) and free profilin (P) in the lower left corner. The reaction can proceed by two routes. Actin may directly elongate the filament ends, or it may first form a complex with profilin (P-A) that binds to the filament end (F_{n+1}-P) followed by the release of profilin (P). The product of the equilibrium constants (K_d or $1/K_d$, depending on the direction of the step, dissociation or association) must be the same for the two routes, i.e., $K_{d1} = c_\infty = K_{dA}K_{d3}/K_{d2}$, in keeping with the law that the free energy change of a reaction is independent of the path of the reaction.

reactions were assumed to depart insignificantly from equilibrium. Thus [P], [P-G], and [P-Y] were calculated as in (c) above. The steady-state assumption yields

$$df_y/dt = k'_{1+}y(1 - f_y - f_{pg} - f_{py}) + (k_{3-}f_{pg} + k'_{3-}f_{py})f_y/(1 - f_{py} - f_{pg}) - (k_{1+}g + k'_{2+}[P] + k_{3+}[P\text{-}G] + k'_{3+}[P\text{-}Y])f_y = 0 \quad (6a)$$

$$df_{py}/dt = k'_{2+}[P]f_y + k'_{3+}[P\text{-}Y](1 - f_{pg} - f_{py}) - (k'_{2-} + k'_{3-})f_{py} = 0 \quad (6b)$$

$$df_{pg}/dt = k_{2+}[P](1 - f_y - f_{pg} - f_{py}) + k_{3+}[P\text{-}G](1 - f_{pg} - f_{py}) - (k_{2-} + k_{3-})f_{pg} = 0 \quad (6c)$$

where f_y = fraction of ends with an uncapped pyrenyl actin; f_{pg} = fraction of ends with a native actin capped by profilin; and f_{py} = fraction of ends with a pyrenyl actin capped by profilin (the remainder, $1 - f_y - f_{pg} - f_{py}$, have an uncapped native actin).

Equations 6b and 6c are linear in f_y, f_{pg}, and f_{py}. Thus for given values of the rate constants and any value of f_y they can be solved simultaneously for f_{pg} and f_{py}, and df_{pg}/df_y and df_{py}/df_y can readily be evaluated. Using this, eq 6a was solved numerically by Newton's method to obtain the correct value of f_y. These equations were in general solved for a series of closely spaced profilin concentrations ranging from zero to the highest level used experimentally. At the lowest nonzero concentration of profilin the iteration was started with f_y set to $y/(g + y)$; for subsequent points the final value at convergence for the previous point was used as a seed.

The observed initial rates of fluorescence change in the presence of profilin were obtained as in (a) above, with the differences that only observations at early times were used, and at least two exponentials were usually needed to fit the experimental fluorescence trajectory. These were then compared graphically with a curve calculated from

$$R_b = s[(k'_{1+}y + k'_{3+}[P\text{-}Y])(1 - f_{pg} - f_{py}) - k'_{1-}f_y - k'_{3-}f_{py}] \quad (7)$$

where s was a scale factor determined from the control rate at zero profilin and the steady-state distribution of the ends over their different forms was estimated as described above. In all cases the values of c_∞, K_{dY}, and K_{dG} were set to those obtained from the relevant controls and sequestration experiments. Native and pyrenyl G-actin addition to filaments were assumed to be diffusion limited, and since low levels of profilin did not significantly change the rate of elongation, the same assumption was made for the addition of P-G and P-Y, except in two cases, one to test this assumption and the other to fit electron microscopy results with native G-actin (Kaiser et al., 1986), as noted in the Results section. In the absence of any contradictory information, this assumption was also made for the on rates of free profilin capping of filaments. The principle of microreversibility was always applied, and so from eqs 4 and 5 only two degrees of freedom remained in choosing the rate constants. These were satisfied by making a range of choices of K_{d2} and K'_{d2} to illustrate the fit of the model to the data, as described in the Results section.

It should be recognized that the above approach to the calculation of expected rates of fluorescence change, even when only initial rates are used, may become inadequate when total free G-actin concentrations in the vicinity of c_∞ are used. This is because under these conditions the effects of small differences between the c_∞ values, or their component rate constants, of native and pyrenyl G-actin, which we always assumed to be equal, could be substantially magnified.

Finally, it should be noted that no analytical solution exists for the full time course of fluorescence change in the presence of profilin under this model. This is because the sequestration constants K_{dG} and K_{dY} differ, and also consequently the pyrenyl labeling of the actin incorporated in filaments will in general differ from that of the added G-actin, so the fractional pyrenylation of all three pools—F-actin, free G-actin, and profilin-sequestered G-actin—will change with time. This explains why the experimental data had to be approximated by multiple exponentials. A complete trajectory of fluorescence change could be calculated by numerical integration, but since it would be at risk of cumulative and increasing errors from the factors outlined in the previous paragraph (approach to c_∞), no attempt was made to do so.

RESULTS

The equilibrium constant for *Acanthamoeba* profilin I binding to *Acanthamoeba* pyrenyl actin was obtained by an indirect method which was applicable because profilin does not bind to the pointed ends of actin filaments (Vandekerckhove et al., 1989). We determined the K_d of profilin for actin monomers from the inhibitory effect of actin sequestration on the pointed end elongation rate of actin filaments which were capped at the barbed ends with gelsolin (Figures 2 and 3), as we have done previously for macrophage capping protein (Young et al., 1990) using the fluorescence change of pyrenyl actin as an indicator for polymerization. However, unlike macrophage capping protein, profilin binds 15- to 20-fold more weakly to pyrenyl than to native actin (Lal & Korn, 1985; Kaiser et al., 1986), making it necessary to estimate two profilin binding constants, for native and for pyrenyl actin, when a mixture of native and pyrenyl actin is used. To solve the two equations for these two unknowns, we used two different ratios of pyrenyl and native actin: 76% pyrenyl actin (Figure 2), the highest ratio available to us in the experimental series described here, and 8.4% pyrenyl actin (Figure 3), the lowest ratio that still gave a reliable signal at the actin concentrations present in these experiments.

We used conventional controls (Young et al., 1990) in the experiments with more or less pure pyrenyl actin (76% shown here and 100% in two other experiments not shown here), i.e.,

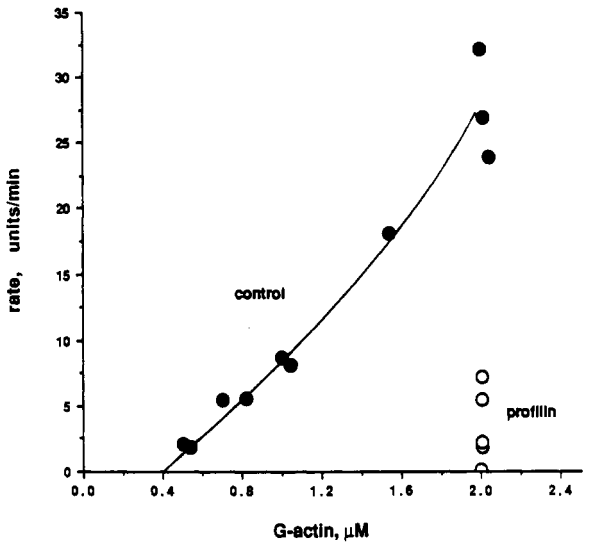

FIGURE 2: Determination of the K_d of profilin for actin monomers. Experiment 1: Inhibition of pointed end elongation by profilin using 76% pyrenyl-labeled actin. Pyrenyl actin was converted from Ca- to Mg-actin by a 20-min incubation with (open circles) or without (closed circles) profilin. Elongation was started by the simultaneous addition of salt, gelsolin-capped actin filaments (actin/gelsolin = 25/1; 200 nM 76% pyrenyl actin), and 15 nM gelsolin–actin dimers to ensure continued complete capping in 1 mM EGTA [capping constant of gelsolin–actin monomers in EGTA is about 0.1 nM as reported by Selve and Wegner (1986)]. Fluorescence was measured continuously for the first 4 min, followed by intermittent readings over most of the time course of the fluorescence increase. For the controls the initial rate was calculated using all data points of the time course which followed a single exponential. In the presence of profilin, when the time course is no longer exponential because of the continuous release of actin from its complex with profilin, the rate was taken from the initial linear part of the time course. The control curve shows data taken on 3 sequential days. The slight curvature of the line connecting the control points (drawn in by hand) has been observed in many experiments over many years (Pollard, 1986; Weber et al., 1987b). The profilin concentrations in order of decreasing rates were 15, 20, 40, and 60 μM.

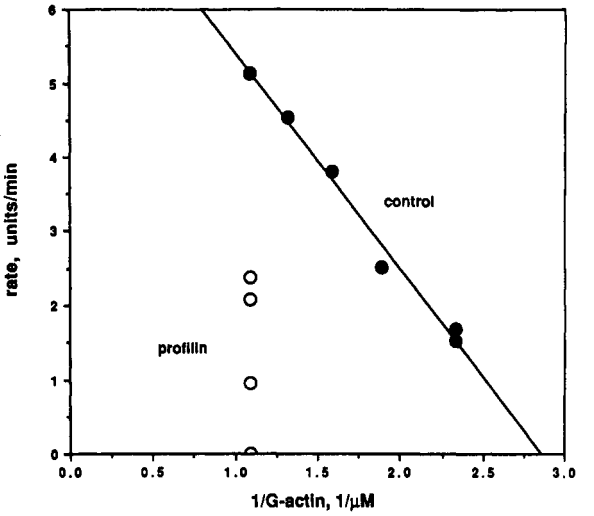

FIGURE 3: Determination of the K_d of profilin for actin monomers. Experiment 2: Inhibition of pointed end elongation using 8.3% pyrenyl-labeled actin. Protocol and symbols as in Figure 2 except that in the controls pyrenyl actin was kept constant at 0.076 μM and the concentration of native actin alone was increased. In the presence of increasing profilin concentrations a constant concentration of 0.9 μM 8.3% pyrenyl-labeled actin was used, and the rates were taken from the initial linear part of the time course. The control elongation rates were plotted against the reciprocal of the total G-actin concentration, which gives a straight line with the abscissa intercept at the critical concentration (cf. eq 1 in the Materials and Methods section). Profilin concentrations were from the top: 1.2, 1.45, 1.67, and 2.9 μM.

rate measurements in the absence of profilin with different concentrations of G-actin and a constant ratio of pyrenyl to native actin. The rates increase in proportion to the G-actin concentration although not in a completely linear fashion (Weber et al., 1987b; Pollard, 1986).

The controls with a small percentage of pyrenyl actin were different; they simulate the events that occur when profilin is added to a mixture of pyrenyl and native actin in concentrations well below its K_d for pyrenyl actin. Under these conditions increasing amounts of profilin added to a mixture of native and pyrenyl actin bind mainly native actin, leaving the pyrenyl actin free. Consequently, the ratio of free pyrenyl to free native actin changes with increasing profilin concentrations (Lal & Korn, 1985), as first pointed out to one of us by E. D. Korn. Therefore, in the control rate measurements only the concentration of native G-actin was increased and the concentration of pyrenyl G-actin was kept constant at 0.076 μM, well below the pointed end critical concentration, so that polymerization and the resulting fluorescence increase could occur only if there was enough native actin to raise the total actin above the critical concentration. With a constant concentration of pyrenyl actin and a decreasing ratio of pyrenyl to native actin, the rate of fluorescence change is no longer a linear function of the total G-actin concentration, but of its reciprocal instead, according to eq 1 in the Materials and Methods section [(a) under "Calculations"]. The rate decreases only by 25% of maximal over the whole range of G-actin concentrations from infinite to 4 times the critical concentration (c_∞). Most of the rate change from 0% to 50% of maximal occurs in the narrow range between c_∞ and $2c_\infty$. The data were analyzed using a graph of the rate versus the reciprocal of the total G-actin concentration (Figure 3). The data in the presence of profilin (Figures 2 and 3) were fitted best (Materials and Methods section, eq 2) with K_{dA} values of 13.8 μM and 0.8 μM for profilin binding to pyrenyl actin and to native actin, respectively (Figure 4). The fit became significantly poorer when the K_d for pyrenyl actin was raised to 20 μM or lowered to 8 μM, or if the K_d for native actin was lowered to 0.4 μM or raised to 3 μM (data not shown). The profilin I preparation from *Acanthamoeba* used for the experiments described here had a higher affinity for native and for pyrenyl actin from *Acanthamoeba* than previously reported (Lal & Korn, 1985; Pollard & Cooper, 1984; Kaiser et al., 1986), and it bound pyrenyl actin 2–3 times more strongly than the preparations used later with 100% pyrene-labeled actin [K_d values of 27 and 43 μM (data not shown)].

We then did the experiment to determine whether profilin–actin complexes contribute to filament elongation at the barbed filament ends. We measured the rate of elongation of *Limulus* acrosomes with 76% pyrenyl actin (Figure 5) (and in later experiments with 100% pyrenyl actin, data not shown) and with native actin spiked with small amounts of pyrenyl actin (Figure 6). Elongation at the pointed end was prevented by keeping the total free G-actin concentration below the critical concentration for the pointed end. The controls were analogous to the controls for pointed end elongation measurements. As explained for the experiments on pointed end elongation, in the control experiments with native actin, pyrenyl actin was kept constant, the concentration of native actin was increased, and the data were plotted as a linear function of the reciprocal of the G-actin concentration (Figure 6). It is evident from the raw data of the experiment with 76% pyrenyl actin (Figure 5) that profilin inhibits the elongation rate much less at the barbed than at the pointed end: 15 μM profilin,

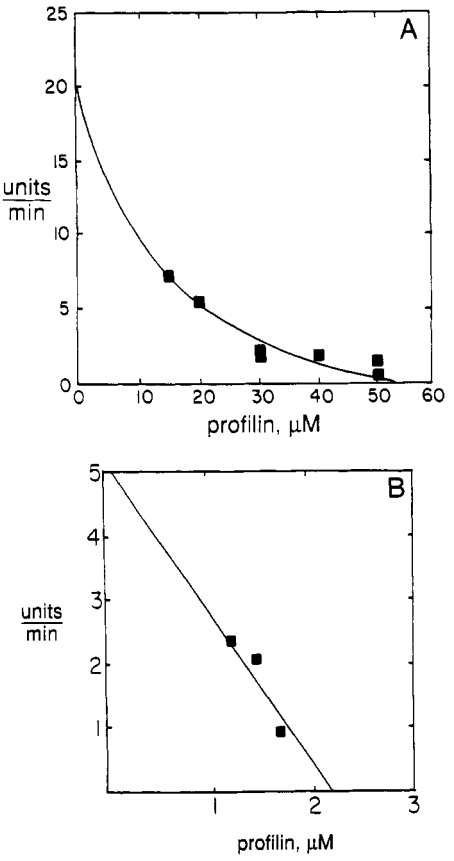

FIGURE 4: Fits of the data points of Figures 2 and 3 with calculated curves. (A) 76% pyrenyl actin; (B) 8.4% pyrenyl actin. Solid squares, data points from Figures 2 and 3. The calculated curves (continuous lines) were drawn with K_{dA} values for monomer sequestration of 0.8 μM and 13.7 μM for native and pyrenyl actin, respectively, and imposing the c_∞ and ak_+n values obtained from the control measurements shown in Figures 2 and 3, as described in the Materials and Methods section.

which sequesters 50% of the pyrenyl actin monomers and more than 90% of the native monomers, did not inhibit measurably. Thus, when these data were plotted against the concentrations of nonsequestered G-actin (Figure 5, open squares), calculated using the K_d's for profilin binding to G-actin obtained from the pointed end measurements (Figures 2–4), the rates were much higher than the control rates in the absence of profilin, indicating that the profilin–actin complexes did contribute to filament elongation at the barbed ends. This contribution declined and eventually ceased at higher concentrations of free profilin so that profilin increasingly inhibited barbed end elongation (cf. Discussion, Figure 10). These results were reproduced with two more, 100% pyrenyl-labeled, preparations. The observations with native actin were comparable. However, with native actin the experimental scatter was relatively large because with increasing actin concentration the rate of pyrenyl fluorescence change increases from 0% to 75% of maximal over a narrow range of very low concentrations between 0.04 and 0.16 μM total G-actin, (1–4) × c_∞ as described above for the determination of the K_d. Furthermore, since the values for native actin can be obtained only if pyrenyl actin is no more than a fraction of the total G-actin, the concentrations of pyrenyl actin in these experiments approached the lower limits of resolution. Nevertheless, for each profilin concentration the rate of elongation was higher than expected for the nonsequestered G-actin, calculated with the K_d values (Figure 4) derived from the experiment of Figure 3. The rate of elongation became zero only at profilin concentrations high enough to lower free G-actin to c_∞. The critical concentration at the

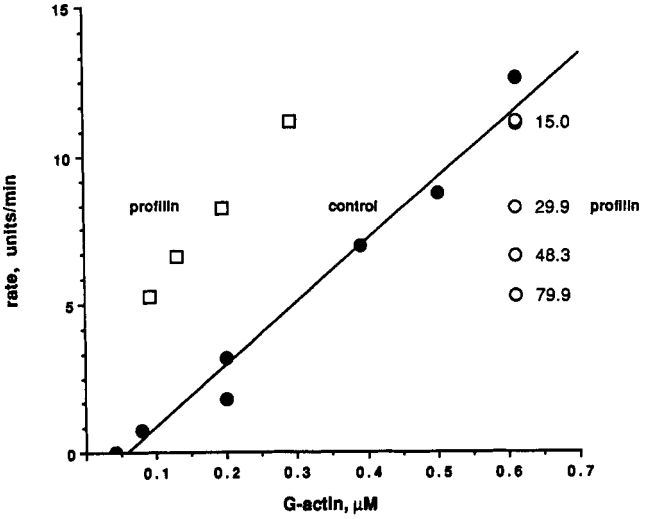

FIGURE 5: Effect of profilin on the barbed end elongation rate using 76% labeled pyrenyl G-actin. General protocol as in Figure 2 except that elongation took place at the barbed ends of *Limulus* acrosomes. The control rates (closed circles) were calculated from the whole time course of elongation, which followed a single exponential. The rates in the presence of profilin were taken from the initial linear portion of the time course. The data in the presence of profilin were plotted against both the total added G-actin (open circles) and the calculated free G-actin (open squares), using the K_d values whose fit is shown in Figure 4A. The profilin concentrations from top to bottom are 15, 29.9, 48.3, and 79.9 μM.

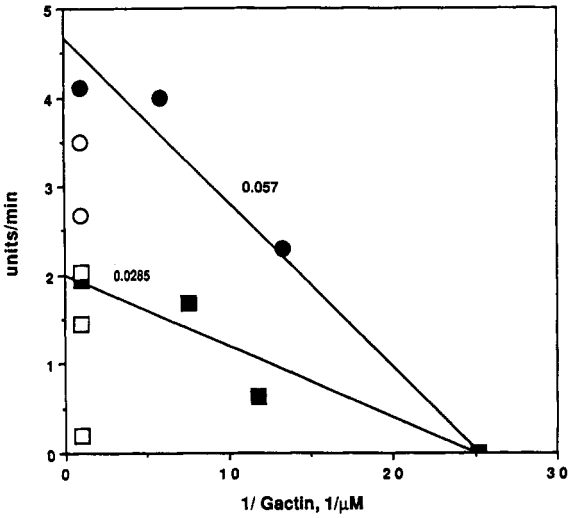

FIGURE 6: Effect of profilin on the barbed end elongation rates using native G-actin spiked either with 0.057 μM or with 0.0285 μM pyrenyl actin. General protocol and presentation as in Figure 3. Controls with a constant concentration of pyrenyl actin: filled circles, 0.057 μM; filled squares, 0.0285 μM. In the presence of profilin a constant concentration of pyrenyl-labeled actin was used, 1.04 μM and 1.08 μM for the 2.85% and 5.7% labeled actin, respectively. In view of the paucity and relatively large scatter of the data two additional constraints were imposed on both lines: (a) the slopes were made to differ by a factor of 2 corresponding to the 2-fold difference in pyrenyl actin, and (b) they were forced to have the same abscissa intercept ($1/c_\infty$). The best value for c_∞ of 0.04 μM is very close to that measured directly, on the same day, for 76% pyrenyl actin which had a value between 0.04 and 0.05 μM. Profilin concentrations used with native actin spiked with 0.057 μM pyrenyl actin (open circles): 7.4 and 37.5 μM; with 0.0285 μM pyrenyl actin (open squares): 14.1, 18.8, and 75 μM.

barbed end was too low and the signal/noise ratio too poor to determine with certainty whether elongation ceased precisely when c_∞ had been reached.

Using the procedure described in Materials and Methods, we then looked for a set of rate constants for profilin–actin

Table I

constants	our data		Kaiser et al.[a]	
	native actin	pyrenyl actin	A	B
K_{dA} (μM)	0.8	13.7	10	10
$K_{d1} = c_\infty$ (μM)	0.035–0.08	0.035–0.08	0.1	0.1
K_{d2} (μM)	1000	1000	1000	1000
K_{d3} (μM)	44–100	2.6–5.8	10	10
k_{1+} (μM^{-1} s^{-1})	10	10	8.3	8.3
k_{2+} (μM^{-1} s^{-1})	10	10	10	0.25
k_{3+} (μM^{-1} s^{-1})	10	10	6.7	8.3
k_{1-} (s^{-1})	0.35–0.8	0.35–0.8	1	1
k_{2-} (s^{-1})	10^4	10^4	10^4	250
k_{3-} (s^{-1})	440–1000	26–58	67	83

[a] The rate constants in columns A and B fit the data of Kaiser et al. equally well. They differ from each other with respect to the values of some of the rate constants: in column A, k_+ for G-actin and for profilin–actin complexes is lower than in column B, and in column B, k_+ and k_- for the binding of profilin alone to the barbed filament end are much lower than in column A and much lower than the constants used on our data.

association and dissociation at the barbed end that would fit the elongation rate measurements at the barbed end and that would result in zero elongation by profilin–actin complexes when the free G-actin had reached the critical concentration (Table I). In other words, we looked for rate constants compatible with the equilibrium at the barbed end described by Figure 1. The justification for an equilibrium approach is given in the Discussion.

K_{dA} and K_{d2} are the K_d's for profilin binding to actin monomers and to barbed filament ends; K_{d3} is the K_d for the binding of profilin–actin to barbed ends. k_{1-}, k_{2-}, and k_{3-} are the corresponding off-rate constants. Briefly, the equilibrium and rate constants were derived as follows (cf. Materials and Methods, under "Calculations" section e, for full details). The values for c_∞ and K_{dA} were measured. The values for K_{d2} and K'_{d2}, the K_d's for profilin binding to native and pyrenyl barbed ends, were found during the fitting procedure for the elongation rates at the barbed end by trial and error. The values for K_{d3} and K'_{d3}, the K_d's for binding of native and pyrenyl profilin–actin complexes to barbed ends, can be calculated using the values of K_{dA}, K_{d2}, and c_∞ as illustrated by the energy square in Figure 1. The on-rate constants for all reactions were assumed to be diffusion limited, i.e., similar to the on-rate constant of actin for the barbed end. The value for k_{3+}, the on-rate constant of the profilin–actin complex, must be very close to the on-rate constant of free actin for the barbed end to be consistent with the rapid rate of elongation at the barbed end in the presence of profilin. In the absence of contrary information, k_{1+} and k_{2+} were assumed to have values of 10 μM^{-1} s^{-1}. The off-rate constants were calculated on the basis of the equilibrium and the on-rate constants.

Figure 7 shows the fit of the model with these rate constants (Table I, our data) to the 76% pyrenyl actin data. The fits to the data at lower pyrenyl contents (data not shown) were adequate in light of the relative paucity and scatter of the points and the fact that in some of them the free G-actin concentrations were close to c_∞. We checked the limits for the two most important constants. The on-rate constant of profilin–actin for the barbed end cannot be significantly lower than that of actin alone. Lowering it to half the constant for free G-actin made the fit very poor (data not shown). The limits for the K_d of profilin binding to the barbed end are much less narrow. However, lowering the K_d of profilin binding to pyrenyl barbed ends from 1 mM to 100 μM gave a significantly poorer fit for the elongation rate measurements with 76% pyrenyl actin (Figure 7, curve 2).

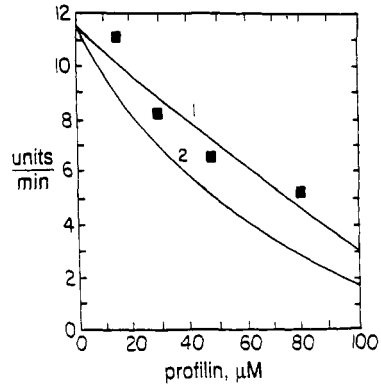

FIGURE 7: Comparison between barbed end elongation rates for 76% pyrenyl actin that were measured with calculated rates using the constants listed in Table I. Solid squares, data of Figure 5. Curve 1, all constants are listed in Table I ("our data"); curve 2, K_d for profilin binding to barbed ends was lowered from 1000 μM to 100 μM.

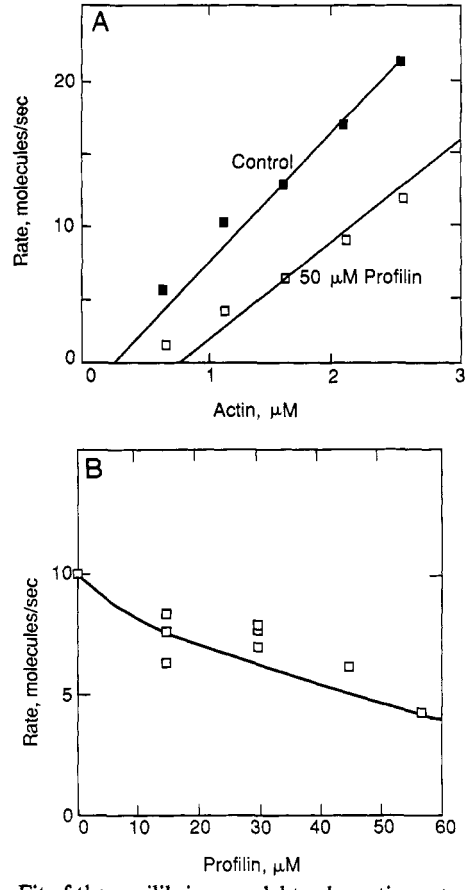

FIGURE 8: Fit of the equilibrium model to elongation rates for pure native actin measured by electron microscopy. The data are taken from Kaiser et al. (1986). (A) Control rates (solid squares) and rates in the presence of 50 μM profilin (open squares). (B) Increasing profilin and constant actin [concentration not stated; assuming k_+ for actin was the same as in (A), the concentration was 1.3 μM]. The curves in (A) and the continuous curve in (B) were calculated using the equilibrium model and the values of the constants shown in *either* column A *or* column B of Table I—the results were essentially identical and therefore are superimposed.

Following the suggestion of one of the reviewers, we also investigated whether this equilibrium model could fit the elongation data obtained by electron microscopy with pure native G-actin by Kaiser et al. (1986). In this case (Figure 8A) the rate of elongation was found to increase somewhat less with increasing total [G-actin] in the presence of profilin than in its absence. This would be expected either if the on-rate constant of profilin–actin complexes were propor-

tionately lower than that of actin or if the elongation rate were somewhat limited by the rate of dissociation of profilin after the profilin–actin complexes have associated with the barbed filament end. As shown in Figure 8, good fits to these authors' data were obtained when either the on-rate constant of profilin–actin complexes was reduced to 6.7×10^6 M^{-1} s^{-1} from the measured value of 8.3×10^6 M^{-1} s^{-1} for G-actin or when the off-rate constant of profilin was reduced to 250 s^{-1} from 10^4 s^{-1}, the value used with our data, while keeping the equilibrium constants of all reactions unchanged. The other rate constants are similar to those used to fit our experiments, taking into account a higher value for the critical concentration in the experiments of Figure 8. Applying these rate constants to our data makes the fit of the model to them poorer (data not shown), suggesting a difference between actin and profilin preparations within the range often encountered.

Discussion

Evaluation of the Data. The primary object of this study was to reinvestigate the contested (Lal & Korn, 1985) finding that profilin–actin complexes elongate actin filaments at the barbed but not at the pointed ends (Pollard & Cooper, 1984; Kaiser et al., 1986) and to examine whether this effect could be explained by a mechanism that did not require input of free energy, e.g., from ATP hydrolysis. We worked with protein preparations similar to those used by Lal and Korn, and we employed comparable optical methods, substituting fluorescence changes of nearly fully and fully pyrenyl-labeled actin for light scattering, since light scattering is at the lower limit of resolution at actin concentrations below the critical concentration for the pointed end.

We obtained reproducible results with three preparations, the 76% labeled actin described here and two more 100% labeled actins, showing that profilin–actin complexes elongate actin filaments at the barbed, but not at the pointed ends, with a similar rate constant as does free G-actin. This confirms for pyrenyl actin what Pollard and his collaborators had observed for native actin. We present here the experiments with 76% labeled pyrenyl and native actin because these data permit the estimation of a complete set of binding and rate constants for labeled and native actin from the same protein preparation.

The data for pyrenyl actin are more accurate than those for native actin which were collected to improve the analysis of the 76% labeled actin, and some of which are relatively sparse and scattered. (The K_d values of profilin for native actin have a higher accuracy than the rate constants for barbed end elongation because the K_d values were obtained at higher actin concentrations in keeping with the higher critical concentration for the pointed end.) To compensate for the shortcoming of our results with native actin, we also analyzed the data of Kaiser et al. (1986) for pure native actin (Figure 8).

The Equilibrium Model for Barbed End Elongation by Profilin–Actin Complexes. We chose to investigate whether an equilibrium model is compatible with our results and those of Kaiser et al. (1986), although filament elongation by G-(ATP)-actin is known to be accompanied by ATP hydrolysis. We justify this on the basis of the observation that under certain conditions the hydrolysis of the terminal phosphate bond does not make any contribution to the free energy of binding of ATP-actin to the barbed filament end. At high inorganic phosphate levels the critical concentrations of ADP-actin and ATP-actin at the barbed end are identical (Rickard & Sheterline, 1986; Wanger & Wegner, 1987; Carlier & Pantaloni, 1988). Furthermore, high phosphate does not affect the binding constant of ATP-actin for the barbed end; rather it increases the binding constant, i.e., lowers the

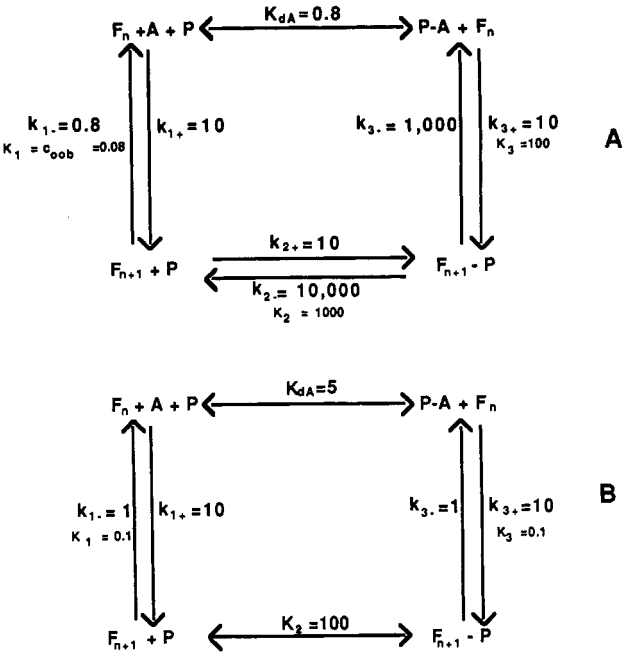

FIGURE 9: Energy squares. The concept of the energy square is explained in the legend of Figure 1. All concentrations refer to μM, and all rate constants are given in s^{-1}. The rate constants appear in larger type than the equilibrium constants. The values apply to native actin used in our experiments; c_∞ is the value observed most often. A brief summary of how the values for energy square A were derived is given in the text for Table I. Energy square B shows the rate constants used by Pollard and Cooper to fit their data to a kinetic model, to which Kaiser et al. (1986) refer.

critical concentration, of ADP-actin. It should be noted, however, that even if there were an energy contribution from ATP hydrolysis, a model of identical form would be valid as long as the contribution of free energy is the same for elongation by free G-actin and by profilin–actin complexes. If this should prove to be the case, it would perhaps best be termed a quasi-equilibrium model.

Our results and those of Kaiser et al. (1986) are compatible with an equilibrium model for profilin–actin interactions, i.e., a model that does not require input of free energy from ATP hydrolysis to drive filament elongation. Filaments are elongated at their barbed ends by free G-actin and by profilin–actin complexes until equilibrium has been reached between the barbed ends, G-actin, profilin–actin complexes, and free profilin. By contrast, the model proposed by Pollard and Cooper (1984), which explains the kinetics of the reactions, requires energy input, presumably from the free energy of ATP hydrolysis, a point not explicitly stated in their paper. Their model also predicts that in the presence of profilin elongation of the filaments would occur at free G-actin concentrations well below the critical concentration in the absence of profilin, an effect that has not so far been observed.

The models are best visualized with a reaction square (Figure 9). The K_d values of Figure 9A, an energy square, obey the thermodynamic constraints of a series of reactions that can be in equilibrium with each other. We show the K_d values and rate constants obtained for native rather than pyrenyl actin because of the much greater interest in these numbers. The equilibrium constants of Figure 9B from the paper by Pollard and Cooper (1984) are the values they used to fit their results and to which Kaiser et al. (1986) refer.

The reaction sequence shows that, starting with G-actin and profilin, the barbed end may incorporate an actin monomer ($F_n \rightarrow F_{n+1}$) by one of two routes. In the simpler one the G-actin binds to the filament end in the normal way without

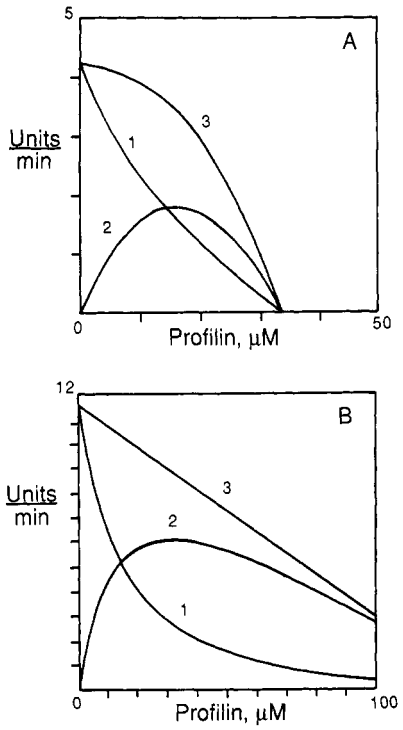

FIGURE 10: Separate contributions of free G-actin (curves 1) and of the profilin–G-actin complexes (curves 2) and their sum (curves 3) to the rate of fluorescence change as a function of profilin concentration. (A) 5.7% pyrenyl actin; (B) 76% pyrenyl actin.

any contribution by profilin. Or it can react with profilin (P) to form a profilin–actin complex (P-A) that binds to the filament end (F_{n+1}-P) and then releases the profilin (P), leaving the actin molecule on the filament (F_{n+1}). If the system is capable of coming to a thermodynamic equilibrium (energy square, Figure 9A), the net free energy change is independent of the route, i.e., the products of the equilibrium constants of each of the two routes must be the same (using the values for either K_d or $1/K_d$ depending on the direction of the reaction: whether it is toward association or toward dissociation), and so $c_\infty = K_{dA}K_{d3}/K_{d2}$. In this case elongation takes place when the concentrations of G-actin and the profilin–actin complexes are higher than their equilibrium values, which means that free G-actin is above the critical concentration for the barbed end. The concentration of profilin is lower than at equilibrium, so that profilin added to the barbed end as the profilin–actin complex dissociates as free profilin from the barbed end, leaving the actin behind and allowing the next profilin–actin complex to bind. Provided the on-rate constant for the profilin–actin complexes is as fast as that for free G-actin and the off-rate constant of profilin is not rate limiting, the initial rate of elongation by profilin–actin complexes can be similar to that of an equal concentration of free G-actin (Figure 10).

Figure 10 shows the contributions of free G-actin (curve 1) and profilin–actin complexes (curve 2) to the total rate of fluorescence increase (curve 3) for our experiment with 5.7% pyrenyl actin (Figure 10A) and with 76% pyrenyl actin (Figure 10B), as a function of profilin concentration. At low profilin levels the rate of elongation by profilin–actin complexes increases as profilin is increased, compensating for the decrease in the concentration of free G-actin, almost completely in Figure 10A, and somewhat less so in Figure 10B. When the profilin concentration is increased further and approaches the equilibrium value, the rate of elongation by profilin–actin complexes reaches a peak and then declines. In other words, profilin increasingly inhibits elongation at the barbed end. The rate of elongation by profilin–actin complexes becomes zero at equilibrium when the free G-actin concentration has been reduced to c_∞. At this point, net flux through each branch of the reaction square is zero.

A high-affinity profilin–actin complex with a K_{dA} of 0.01 μM (Mc Leod et al., 1989) has been isolated from spleen (Carlsson et al., 1977), macrophages (Southwick & Young, 1990), and platelets (Lind et al., 1987). Within the constraints of the equilibrium model the high-affinity profilin–actin complex cannot make as great a contribution to the elongation of barbed filament ends, since it does so with a much lower rate than a comparable concentration of the low-affinity complex described in this paper. This follows from the expression $c_\infty/K_{dA} = K_{d3}/K_{d2} = 10$ for the high-affinity complex. Consequently, K_{d3} of the high-affinity complex for the barbed end is 10 times higher than K_{d2} of profilin alone for the same site. Therefore (with constants maximizing the contribution to the elongation rate) the off-rate constant of the profilin–actin complex is 10-fold higher than that of profilin. As a result, the rate of elongation is limited by the rate of profilin dissociation from the barbed end. Nevertheless, if the concentration of free G-actin is low (e.g., 0.5 μM, the steady-state concentration when all barbed ends are capped) a high concentration of the high-affinity profilactin complex, e.g., 50 μM, could increase the initial rate of elongation by nearly 10-fold over that due to free G-actin, if free barbed ends suddenly became available for elongation.

It can be seen from Figure 9A that profilin should also affect the depolymerization rate if this equilibrium model is correct. The rate constants in Figure 9A show that the profilin–actin complex at the barbed end has a higher off-rate constant than actin alone. Therefore, profilin would be expected to increase the rate of depolymerization from the barbed end when free G-actin is below the critical concentration, and when free profilin concentrations are sufficiently high to combine with the barbed ends to a significant degree. Profilin-bound actin should dissociate with the high rate constant of the profilin–actin complex, followed by rebinding of another free profilin molecule to the barbed end and the dissociation of another profilin-bound actin molecule. However, this applies only to equilibrium conditions, i.e., the terminal actin molecule at the barbed end should contain the same nucleotide as during elongation, presumably ATP or ADP·P, and not ADP, the normal terminal nucleotide under depolymerizing conditions [cf. Carlier (1991) and Pollard (1986)]. Therefore, we have tried to saturate the terminal actin molecule with ADP·P during depolymerization by the addition of high concentrations of inorganic phosphate as described by Carlier (1991). We found that in the presence of 100 mM phosphate profilin did not significantly increase the rate of depolymerization from the barbed ends (data not shown). However, since it has never been proved that added phosphate binds to the active site (Wanger & Wegner, 1986), this finding cannot be clearly interpreted. Final proof for the validity of the equilibrium model can only be made in the absence of an energy source. Therefore, we intend to continue these studies with ADP-actin in the absence of ATP.

Regardless of the mechanism, the ability of profilin–actin complexes to elongate actin filaments at the barbed end could be of considerable biological significance, possibly adding another important function of profilin to those already known (Lassing & Lindberg, 1985, 1988; Goldschmidt-Clermont et al., 1990, 1991). A sudden increase in intracellular polymerized actin might be a consequence of the sudden availability of free barbed ends. This results in an increase in the extent

of polymerization regardless of whether the profilin–G-actin complex can participate in filament elongation. G-Actin is incorporated at the barbed ends because free G-actin at the critical concentration for pointed ends (0.5 μM) is above the critical concentration for barbed ends. With increasing conversion of G- to F-actin, profilin–actin complexes at equilibrium with the higher free G-actin dissociate, releasing more free G-actin for filament elongation. Elongation proceeds until free G-actin has been lowered to the critical concentration for filaments with free barbed ends (0.1 μM). However, the rate of elongation is slow if only free G-actin associates with the filaments because the steady-state free G-actin concentration is so low. Direct filament elongation by the profilin–actin complex could increase the rate of elongation in a cell by about 50-fold, assuming the concentration of the low-affinity profilin–actin complex discussed here is 50-fold greater than the free G-actin concentration, i.e., about 25 μM as compared to 0.5 μM free G-actin. Thus the ability of profilin–actin to elongate actin filaments rapidly suggests that uncapping alone can result in a high rate of elongation and that there may be no need for the release of a large concentration of free G-actin which would require an additional regulatory event, such as the inactivation of one or more actin monomer binding proteins.

ACKNOWLEDGMENTS

We thank Dr. Edward Korn warmly for valuable discussions with regard to the experimental approach and its possible pitfalls and for his support for this work. We are much indebted to Dr. Peter Lambooy for providing us with *Acanthamoeba* actin and profilin for the early experiments, and we thank Dr. Joseph Bryan for a generous gift of plasma gelsolin and Dr. Mark Mooseker for providing us with the villin used in the depolymerization experiments.

Registry No. ATP, 56-65-5.

REFERENCES

Bamberg, J. R., Harris, H. E., & Weeds, A. G. (1980) *FEBS Lett. 121*, 178–181.
Bryan, J. (1988) *J. Cell Biol. 106*, 1553–1562.
Bubb, M. R., & Korn, E. D. (1991) *Methods Enzymol. 196*, 119–125.
Bubb, M. R., Lewis, M. S., & Korn, E. D. (1991) *J. Biol. Chem. 266*, 3820–3826.
Carlier, M. F. (1991) *J. Biol. Chem. 266*, 1–4.
Carlier, M. F., & Pantaloni, D. (1988) *J. Biol. Chem. 263*, 817–825.
Carlier, M. F., Pantaloni, D., & Korn, E. D. (1986) *J. Biol. Chem. 261*, 10785–10792.
Carlson, M., Weber, A., & Zigmond, S. H. (1986) *J. Cell Biol. 103*, 2707–2714.
Carlsson, L., Nystrom, L. E., Sundkvist, I., Markey, F., & Lindberg, U. (1977) *J. Mol. Biol. 115*, 465–483.
Casella, J. F., Flanagan, M. D., & Lin, S. (1981) *Nature 293*, 302–305.
Cooper, J. A., Blum, J. D., Williams, R. C., Jr., & Pollard, T. D. (1986) *J. Biol. Chem. 261*, 477–485.
Devriotes, P., & Zigmond, S. H. (1988) *Annu. Rev. Cell Biol. 4*, 649–686.
Fecheimer, M., & Zigmond, S. H. (1983) *Cell Motil. 3*, 349–361.
Fox, J. E. B., & Phillips, D. R. (1981) *Nature 292*, 650–652.
Goldschmidt-Clermont, P. J., Machesky, L. M., Baldassare, J. J., & Pollard, T. D. (1990) *Science 247*, 1575–1578.
Goldschmidt-Clermont, P. J., Kim, J. W., Machesky, L. M., Rhee, S. G., & Pollard, T. D. (1991) *Science 251*, 1231–1233.
Gordon, D. J., Boyer, J. L., & Korn, E. D. (1977) *J. Biol. Chem. 252*, 8300–8309.
Kaiser, D. A., Sato, M., Ebert, R. F., & Pollard, T. D. (1986) *J. Cell Biol. 102*, 221–226.
Kitasawa, T., Shuman, H., & Somlyo, A. P. (1982) *J. Muscle Res. Cell Motil. 3*, 437–454.
Korn, E. D. (1982) *Physiol. Rev. 62*, 672–737.
Kouyama, T., & Mihashi, K. (1981) *Eur. J. Biochem. 114*, 33–38.
Lal, A. A., & Korn, E. D. (1985) *J. Biol. Chem. 260*, 10132–10138.
Lambooy, P. K., & Korn, E. D. (1986) *J. Biol. Chem. 261*, 17150–17155.
Lassing, I., & Lindberg, U. (1985) *Nature 314*, 472.
Lassing, I., & Lindberg, U. (1988) *J. Cell Biochem. 37*, 255.
Lind, S. E., Janmey, P. A., Chaponier, C., Herbert, T. J., & Stossel, T. P. (1987) *J. Cell Biol. 105*, 833–842.
Mabuchi, I. (1983) *J. Cell Biol. 97*, 1612–1621.
Mc Leod, J. F., Kowalski, M. A., & Haddad, J. G., Jr. (1989) *J. Biol. Chem. 264*, 1260–1267.
Mockrin, S. C., & Korn, E. D. (1980) *Biochemistry 19*, 5359–5362.
Moriyama, K., Nishida, E., Yonezawa, N., Sakai, H., Matsumoto, S., Iida, K., & Yahara, I. (1990) *J. Biol. Chem. 265*, 5768–5773.
Newman, J., Estes, E. J., Selden, L. A., & Gershman, L. C. (1985) *Biochemistry 24*, 1538–1544.
Northrop, J., Weber, A., Mooseker, M. S., Franzini-Armstrong, C., Bishop, M. F., Dubyak, M. F., Tucker, M., & Walsh, T. P. (1986) *J. Biol. Chem. 261*, 9274–9281.
Pantaloni, D., Hill, T. L., Carlier, M. F., & Korn, E. D. (1985) *Proc. Natl. Acad. Sci. U.S.A. 82*, 7207–7211.
Pardee, J. D., & Spudich, J. A. (1982) *J. Cell Biol. 93*, 648–654.
Pollard, T. D. (1986) *J. Cell Biol. 103*, 2747–2754.
Pollard, T. D., & Cooper, J. A. (1984) *Biochemistry 23*, 6631–6641.
Pollard, T. D., & Weeds, A. G. (1984) *FEBS Lett. 170*, 94–96.
Pollard, T. D., & Cooper, J. A. (1986) *Annu. Rev. Biochem. 55*, 987–1035.
Reichstein, E., & Korn, E. D. (1979) *J. Biol. Chem. 254*, 6174–6179.
Rickard, J. E., & Sheterline, P. (1986) *J. Mol. Biol. 191*, 273–280.
Safer, D., Gola, R., & Nachmias, V. T. (1990) *Proc. Natl. Acad. Sci. U.S.A. 87*, 2536–2540.
Safer, D., Elzinga, M., & Nachmias, V. T. (1991) *J. Biol. Chem. 266*, 4029–4032.
Selden, L. A., Estes, J. E., & Gershman, L. C. (1983) *Biochem. Biophys. Res. Commun. 116*, 478–485.
Selve, N., & Wegner, A. (1986) *J. Mol. Biol. 187*, 627–631.
Southwick, F. S., & Young, C. L. (1990) *J. Cell Biol. 110*, 1965–1973.
Tilney, L. G. (1975) *J. Cell Biol. 64*, 289–310.
Tilney, L. G., Bonder, E. M., Coluccio, L. M., & Mooseker, M. S. (1983) *J. Cell Biol. 97*, 112–124.
Tobacman, L. S., & Korn, E. D. (1982) *J. Biol. Chem. 257*, 4166–4170.
Tobacman, L. S., Brenner, S. L., & Korn, E. D. (1983) *J. Biol. Chem. 258*, 8806–8812.

Tseng, P. C., & Pollard, T. D. (1982) *J. Cell Biol. 94*, 213-218.
Tseng, P. C., Runge, M. S., Cooper, J. A., Williams, R. C., Jr., & Pollard, T. D. (1984) *J. Cell Biol. 98*, 214-221.
Vandekerckhove, J. S., Kaiser, D. A., & Pollard, T. D. (1989) *J. Cell Biol. 109*, 619-626.
Vandekerckhove, J. S., Van Damme, J., Vancompernolle, K., Bubb, M. R., Lambooy, P. K., & Korn, E. D. (1990) *J. Biol. Chem. 265*, 12801-12805.
Wallace, P. J., Wersto, R. P., Packman, C. H., & Lichtman, M. A. (1984) *J. Cell Biol. 99*, 1060-1065.
Walsh, T. P., Weber, A., Higgins, J., Bonder, E. M., & Mooseker, M. S. (1984) *Biochemistry 23*, 2613-2621.
Wanger, M., & Wegner, A. (1987) *Biochim. Biophys. Acta 914*, 105-113.
Weber, A., Herz, R., & Reiss, I. (1960) *Biochemistry 8*, 2266-2271.
Weber, A., Northrop, J., Bishop, M. F., Ferrone, F. A., & Mooseker, M. S. (1987a) *Biochemistry 26*, 2528-2536.
Weber, A., Northrop, J., Bishop, M. F., Ferrone, F. A., & Mooseker, M. S. (1987b) *Biochemistry 26*, 2537-2544.
Young, C. L., Southwick, F. S., & Weber, A. (1990) *Biochemistry 29*, 2232-2240.

Actomyosin Interactions in the Presence of ATP and the N-Terminal Segment of Actin†

Gargi DasGupta and Emil Reisler*

Department of Chemistry and Biochemistry and Molecular Biology Institute, University of California, Los Angeles, California 90024

Received September 13, 1991; Revised Manuscript Received November 8, 1991

ABSTRACT: The binding of myosin subfragment 1 (S-1) to actin in the presence of ATP and the acto–S-1 ATPase activities of acto–S-1 complexes were determined at 5 °C under conditions of partial saturation of actin, up to 90%, by antibodies against the first seven N-terminal residues on actin. The antibodies [$F_{ab}(1-7)$] inhibited strongly the acto–S-1 ATPase and the binding of S-1 to actin in the presence of ATP at low concentrations of S-1, up to 25 μM. Further increases in S-1 concentration resulted in a partial and cooperative recovery of both the binding of S-1 to actin and the acto–S-1 ATPase while causing only limited displacement of $F_{ab}(1-7)$ from actin. The extent to which the binding and the ATPase activity were recovered depended on the saturation of actin by $F_{ab}(1-7)$. The combined amounts of S-1 and F_{ab} binding to actin suggested that the activation of the myosin ATPase activity was due to actin free of F_{ab}. Examination of the acto–S-1 ATPase activities as a function of S-1 bound to actin at different levels of actin saturation by $F_{ab}(1-7)$ revealed that the antibodies inhibited the activation of the bound myosin. Thus, the binding of antibodies to the N-terminal segment of actin can act to inhibit both the binding of S-1 to actin in the presence of ATP and a catalytic step in ATP hydrolysis by actomyosin. The implications of these results to the regulation of actomyosin interaction are discussed.

Kinetic schemes for the hydrolysis of ATP by actomyosin predict the existence of two groups of states for the binding of myosin cross-bridges to actin. The "weak-binding" states are identified with M·ATP and M·ADP·P_i complexes, while the "strong-binding" states describe the interactions of myosin and actin in the absence of nucleotides or in the presence of ADP, PP_i, adenyl-5′-yl imidodiphosphate and (AMP·PNP)[1] (Brenner, 1990). Stiffness measurements on muscle fibers confirm the results of kinetic studies in solution and provide evidence for "weak-binding" (Schoenberg, 1988) and "strong-binding" (Brenner et al., 1986) cross-bridge states in muscle. It is expected that the large differences between these states in the affinities of myosin for actin have a structural basis and that the transition between the different structures is important for the power stroke in muscle. Indeed, X-ray diffraction studies (Yu & Brenner, 1987; Harford & Squire, 1990), electron microscopy (Craig et al., 1985; Applegate & Flicker, 1987; Frado & Craig, 1991), and solution studies (Bernett & Thomas, 1989; Duong & Reisler, 1989; Trayer & Trayer, 1988) attest to significant conformational differences between myosin heads (S-1) bound strongly and weakly to actin.

Further progress in understanding the structure and function of different cross-bridge states should be facilitated by a recent determination of the atomic resolution structure of G-actin (Kabsch et al., 1990), the refined models of F-actin (Holmes et al., 1990; Milligan et al., 1990), and advances in the mapping of actomyosin binding sites (Labbe et al., 1990). Two binding sites, one on S-1 and one on actin, merit special attention in the context of state-specific actomyosin interactions. On the S-1, several residues around the reactive SH_1 cysteine have been implicated in the formation of the strong actomyosin bond (Suzuki et al., 1987; Keane et al., 1990). However,

† This work was supported by Grant AR 22031 from the National Institutes of Health and Grant DMB 89-05363 from the National Science Foundation.

[1] Abbreviations: S-1, myosin subfragment 1; S-1·T, S-1 in the presence of MgATP; $F_{ab}(1-7)$, affinity-purified F_{ab} fragment of polyclonal peptide antibodies raised against the first seven N-terminal residues of α-skeletal actin; AMP·PNP, adenyl-5′-yl imidodiphosphate; ELISA, enzyme-linked immunosorbent assay; SDS–PAGE, sodium dodecyl sulfate–polyacrylamide gel electrophoresis.

0006-2960/92/0431-1836$03.00/0